Original Paper

Cellular Physiology and Biochemistry

Cell Physiol Biochem 2009;24:53-64

Accepted: May 15, 2009

cAMP-Dependent Chloride Conductance Evokes Ammonia-Induced Blebbing in the Microglial Cell Line, BV-2

Nina Svoboda[1,3], Sylvia Pruetting[2,3], Stephan Grissmer[2] and Hubert H. Kerschbaum[1]

[1]Department of Cell Biology, University of Salzburg, [2]Institute of Applied Physiology, University of Ulm, [3]contributed equally to this study

Key-Words

Cell blebbing • Chloride conductance •cAMP • Apoptosis • Microglia • Ammonium

Abstract

Cell blebbing is a key feature in apoptosis. Because blebbing dynamically alters cell volume and regulatory volume changes have been linked to chloride (Cl) channels, we evaluated an association between blebbing and Cl channels activity. We used scanning electron microscopy, confocal laser microscopy, and cell sorting to quantify cell volume and blebbing and whole-cell recording to characterize Cl^- currents. We found that blockade of Cl channel activity as well as inhibition of adenylyl cyclase or protein kinase A (PKA) activity suppressed ammonia-induced blebbing in the microglia cell line, BV-2. In further experiments, we elucidated the common mechanism of Cl channel activity and cyclic adenosine 3',5'-monophosphate (cAMP)-dependent pathway on cell blebbing. These experiments indicated that perfusion of cells with cAMP or the catalytic subunit of PKA activated a Cl^- current under normotonic conditions. The pharmacological profile (sensitivity to 5-nitro-2-(3-phenylpropylamino)benzoic acid [NPPB], flufenamic acid, and [(dihydroindenyl)oxy]alkanoic acid [DIOA]), outward rectification, and kinetic of the current were identical to the swelling-activated Cl channel. Superfusion of cells with ammonia elicited an outwardly rectifying current sensitive to Cl channel blockers. We propose that ammonia induces a PKA-dependent phosphorylation of Cl channels. Localized influx of Cl^- is followed by influx of water, required for bleb expansion.

Introduction

Microglial, brain-resident monocyte-derived cells, are polymorphic cells, which vary along a continuous gradient from an amoeboid to a ramified phenotype [1-3]. Ramified phenotypes continuously survey the environment with their cellular processes for the integrity of blood vessels or presence of pathogens [4, 5], whereas amoeboid phenotypes migrate through brain parenchyma and phagocyte pathogens as well as cell debris, which accumulate during development of the brain or neurodegenerative processes in the mature brain, like multiple sclerosis [6, 7].

KARGER

Fax +41 61 306 12 34
E-Mail karger@karger.ch
www.karger.com

1015-8987/09/0242-0053$26.00/0

Accessible online at:
www.karger.com/cpb

Hubert H. Kerschbaum
Division of Animal Physiology
Department of Cell Biology, University of Salzburg
Hellbrunnerstr. 34, 5020 Salzburg (Austria)
Fax +43-662-8044-180, E-Mail hubert.kerschbaum@sbg.ac.at

Microglial cells employ local protrusions in several cellular responses, like initialization of ramifications, extension of lamellipodia, formation of engulfment pseudopodia upon phagocytosis, or blebbing in the early phase of apoptosis [8-13]. A common denominator of cellular volume changes is the activation of swelling-activated Cl channels. Accordingly, Cl channels have been found to participate in ramification, lamellipodium formation, migration, and phagocytosis [8-13]. However, the sequence of events is less clear. E.g., what is first, a volume increase, which activates Cl channels or an increase in Cl^- conductance, which leads to a volume increase? Placing an increase of Cl^- conductance before volume increase requires (1) an intracellular factor, which activates Cl channels, and (2) an exogenous factor, which delivers a signal for an increase in this intracellular factor.

In the present study, we propose that cyclic adenosine 3',5'-monophosphate (cAMP) facilitates activation of Cl channels. A cAMP-dependent Cl^- current has been reported in rat carotid body type I cells [14] and rat hepatocytes [15]. Because we have found that intracellular cAMP is increased during ammonia-induced apoptosis [10] and apoptosis is accompanied by intense blebbing, we were interested, whether cAMP contributes to Cl^- conductance and, consequently, water influx and local swellings.

We suggest that blebbing is the result of dynamic intracellular processes driven by local interactions between cAMP generation, Cl channel activation and water influx. This assumption is based on our identification of a cAMP-dependent Cl^- current and on the finding that inhibition of Cl channels by Cl channel blockers or prevention of Cl channel activation by inhibition of adenylyl cyclase and cAMP-dependent protein kinase (protein kinase A, PKA), respectively, minimizes ammonia-induced bleb formation. As conventional in the literature, "ammonia" will be used inclusively to mean the total of ammonium, NH_4^+, and its conjugate base ammonia, NH_3.

Materials and Methods

Cell culture and reagents

Cells of the murine microglial cell line, BV-2, were maintained in 25cm² culture flasks in Dulbecco's modified Eagle's medium (DMEM) supplemented with 2200mg glucose/L and 10% fetal calf serum (Gibco/BRL Life Technologies, Gaithersbury, MD, USA) at 37°C in a humidified atmosphere of 5% CO_2. BV-2 cells were sub-cultured twice a week. Cells were replaced with fresh ones from frozen stocks of an early passage every three months. For experiments, BV-2 cells were seeded into Petri dishes and initially incubated for 14 hours in the presence of 10% serum to promote adhesion. Following two washes in serum-free DMEM, cells were treated with different reagents in serum-free DMEM. Prior to the treatment of cells with an inhibitor in the presence of ammonia, cells were incubated for 30 minutes with the inhibitor only.

Unless otherwise stated, all reagents were purchased from Sigma-Aldrich (St. Louis, Missouri, USA). The stock solution of (1) ammonia (ammonium chloride, NH_4Cl) (Merck kgaA, Darmstadt, Germany) (1M) was prepared in distilled water, sterile filtrated and stored at 4°C, (2) 8-Br-cAMP (10mg/ml) and Sp-cAMP (1mg/ml) in sterile water and stored at -20°C, (3) SQ-22536 (5mg/ml) in sterile water and stored at 4°C, (4) H-89 (5mg/ml) in sterile water and stored at 4°C, (5) Rp-cAMPs (1mg/ml) in sterile water and stored at -20°C, (6) DIOA (25mM) and flufenamic acid (1M) in ethanol and stored at -20°C, and (7) NPPB (25mg/ml) in dimethyl sulfoxide (DMSO) and stored at -20°C.

All working solutions were made immediately before use, diluted in serum-free DMEM and used at 37°C. To balance osmolarity in extracellular solutions containing 10mM or 30mM NH_4^+, serum-free DMEM was diluted with sterile water and ammonia was added to obtain the desired ammonia concentration and an osmolarity of about 330mosmol.

Flow cytometry

Volume changes during membrane blebbing were investigated via flow cytometry. Cells were seeded into uncoated Petri dishes at a density of $1x10^5$ cells/ml and collected by trypsinization. After centrifugation at 200g for five minutes, cells were resuspended in 500µl of distinct reagents. To avoid the formation of cell pellets during incubation, tubes containing cell suspensions were shaken every 5 minutes. Finally, cell suspensions were analyzed with the FACSCanto™ II Flow Cytometry System (BD Biosciences, San Jose, CA, USA) by measuring forward light scattering. Flow cytometric analysis was performed with Win MDI 2.9 software (free ware).

Scanning electron microscopy

Cells were seeded on poly-D-lysine-coated glass coverslips at a density of $1x10^4$ cells/mL and cultured in Petri dishes. Following incubation with various reagents, cells were fixed in 2.5% glutaraldehyde in phosphate-buffered saline (PBS) for one hour followed by at least three rinses for 15 minutes in PBS and by dehydration in a graded series of ethanol. Thereafter, samples were critical point-dried with a Baltec Critical Point Dryer LPD030 (eleven times for two minutes), coverslips were glued on pins, and cells were sputter-coated with a 50nm layer of gold using an Agar Sputter Coater (15 seconds). Specimens were inspected and photographed with a CAMBRIDGE stereoscan 250 scanning electron microscope. Electron micrographs were digitalized and analyzed by Orion software (ORION™, E.L.I. sprl. Brussels, Belgium).

Time-lapse videomicroscopy

Cells were seeded into Petri dishes on poly-D-lysine-coated glass coverslips (Ø 32mm) at a density of $2x10^4$ cells/ml. Coverslips on which cells had been cultured were affixed onto

the bottom of the laminar fluid flow chamber (Zeiss, Germany). Laminar flow of serum-free DMEM into the flow chamber at a constant rate was created using a syringe pump. A constant fluid level was maintained by aspirating the supernatant via a vacuum pump. The flow chamber was set at a constant temperature of 37°C through an electrical warmer.

Visual evaluation of cells superfused with different reagents was performed by time-lapse video microscopy using a confocal laser scanning microscope (LSM 510 Meta, Zeiss, Germany). Cells were visualized via a Helium Neon laser with an excitation wavelength of 543nm and a plan-apochromat 63 x/1.4 oil DIC objective. Over a period of 30 minutes, every ten seconds a differential interference contrast image was acquired. Images were digitized and evaluation was performed with Zeiss LSM Image Examiner.

Quantification and analysis of the blebbing process was performed using a blebbing index modified from that developed by Charras *et al.* [16]. The blebbing index was computed for each cell at certain points in time as follows:

$$B = \frac{N_{blebs}}{I} \quad (1)$$

N_{blebs} is the number of blebs observed at a certain time and I the perimeter (in µm) of the cell body excluding its blebs. Thus, the blebbing index is the number of blebs divided by the perimeter of the cell.

Electrophysiology

Cells were plated on poly-D-lysine (1mg/ml)-coated glass coverslips. Cl^- currents were monitored in a standard whole-cell recording mode [17-19] with an EPC-9 patch clamp amplifier (HEKA Elektrotechnik, Lambrecht, Germany) connected to a Dell computer running Patchmaster/Fitmaster 2.0 data acquisition and analysis software. All currents were filtered by a 2.9kHz Bessel Filter and recorded with a sampling frequency of 2.0kHz. At the beginning of the experiment, the cell was superfused with standard external solution (see below) using a syringe-driven permanent perfusion system. Swelling-activated Cl^- current was elicited by exposure of the cells to a hypoosmotic solution (60% extracellular saline). Hypoosmotic external solution (60% external saline) was prepared by diluting the external solution with distilled water. Cl^- current was recorded during a 400ms voltage ramp from -120mV to +80mV. Voltage ramps were elicited every 10 seconds. After break-in and formation of stable whole-cell recording mode, membrane and pipette capacitance were compensated using an electronic feedback via the patch clamp amplifier. The holding potential in all experiments was 0mV. Electrodes were pulled from glass capillaries (Science Products, Hofheim, Germany) in three stages and fire-polished. Electrodes filled with internal solution had resistances ranging between 2 and 4MΩ. The internal solution contained (in mM): 150 K-aspartate, 1 $CaCl_2$, 2 $MgCl_2$, 10 HEPES, 10 EGTA, 3 Mg_2ATP, 0.5 GTP; titrated to pH 7.2 with KOH. In some experiments, the internal solution contained cAMP (0.3 or 1.0mM) or the catalytic subunit of PKA (300 units). The external solution contained (in mM): 164.5 NaCl, 2 $CaCl_2$, 1 $MgCl_2$, 5 HEPES; titrated to pH 7.4 with NaOH. The osmolarity of both solutions was adjusted to 300mosmol using distilled water. The external symmetrical Cl^- solution contained (in mM): 114 NaCl, 2 $CaCl_2$, 1 $MgCl_2$, 4 KCl, 1 $BaCl_2$, 10 HEPES; 5mM NaCl were substituted with 5mM NH_4Cl; the internal symmetrical Cl^- solution contained (in mM): 120 CsCl, 11 EGTA, 1 $CaCl_2$, 2 $MgCl_2$, 10 HEPES, 4 NaATP; both solutions were titrated to pH 7.35 using NaOH or CsOH, respectively, and the osmolarity was adjusted to 300mosmol using D(+)-sucrose. Liquid junction potentials between pipette and bath solution (< 5mV) were not corrected. All experiments were done at room temperature. The membrane capacitance was determined before each pulse during the measurements by the patch clamp amplifier via C-slow recording of the Patchmaster software. Further data analysis was performed using the Igor Pro 3.1 (WaveMetrics, Oregon, USA) software package.

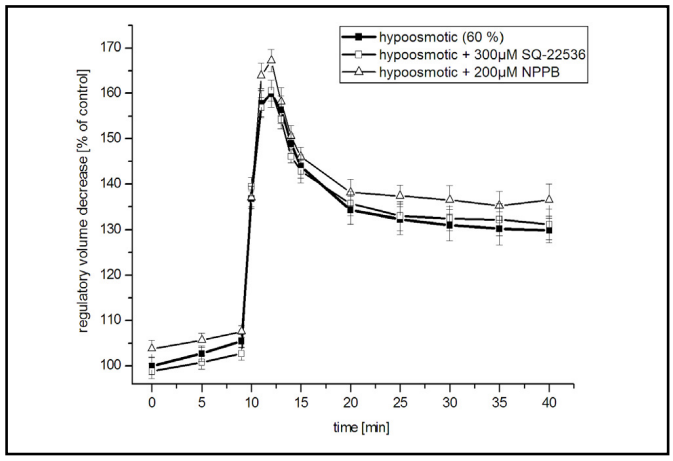

Fig. 1. NPPB delays whereas SQ-22536 does not affect RVD. After incubation of BV-2 cells in normotonic saline in the presence of NPPB (200µM) or SQ-22536 (300µM), respectively, for ten minutes, the cells were exposed to a hypoosmotic solution (60% saline). Cell volume was measured using cell sorting (see Material and Methods). Cells exposed to NPPB showed a moderate, but significant ($p < 0.05$) increase in cell volume under normotonic conditions. In hypoosmotic solution, NPPB-treated cells showed a larger cell volume increase and a delayed RVD than control cells. SQ-22536-treated cells did not differ significantly in cell volume and RVD from control cells. Each data point represents the mean ± SD from four independent experiments.

Results

Inhibition of adenylyl cyclase or PKA activity suppresses ammonia-induced cell swelling and blebbing, respectively

Under physiological conditions, ammonia concentrations in the rodent brain range from 0.1 - 0.3mM [20], but under hyperammonemia, values in the 1 - 5mM range have been reported [21]. Our previous study showed that ammonia increased cAMP and blockade of a cAMP-dependent pathway prevented ammonia-induced

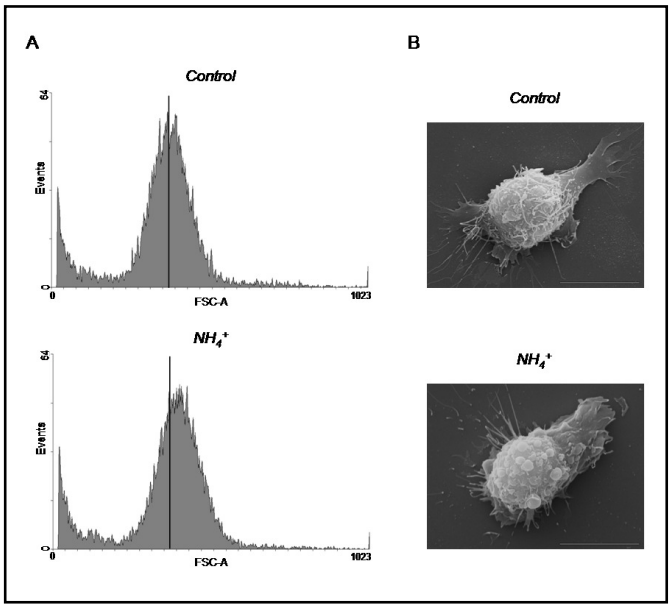

Fig. 2. Ammonia increases cell volume. Cells were cultured in serum-free medium in the absence (control) or presence of ammonia (10mM) for 25 minutes. Cell volume was quantified using cell sorting (see Material and Methods) (A) and cell blebbing was visualized via scanning electron microscopy (B). B: Scale bar, 10µm.

apoptosis in BV-2 cells [10]. Because membrane blebbing is an apoptotic feature, we investigated the effect of the cAMP-dependent pathway on membrane blebbing.

BV-2 cells responded to a hypoosmotic challenge (60%) with an increase of their cell volume by 160 ± 3% (four independent experiments; 10 000 cells each) (Fig. 1). They reached their maximum volume within three minutes. Osmotic challenge in the presence of 5-nitro-2-(3-phenylpropylamino)benzoic acid (NPPB) (200µM) elicited a significantly larger swelling (167 ± 2%; $p < 0.01$) and delayed the regulatory volume decrease (RVD) (Fig. 1). Exposure of BV-2 cells to NPPB in normotonic saline increased their volume by 106 ± 2% ($p < 0.05$). This effect was significant and indicated that Cl channels may continually survey the cell volume. Next, we evaluated the impact of the cAMP pathway on the RVD. Pre-exposure of BV-2 cells to the adenylyl cyclase inhibitor, SQ-22536 (300µM), did neither affect magnitude nor RVD (Fig. 1).

Exposure of cells to ammonia (10mM) for 25 minutes increased cell volume by about 110 ± 2% (Fig. 2A). Cell swelling could be a consequence of an intracellular accumulation of ammonia [22]. However, in addition to this global effect, ammonia promoted formation of numerous blebs (Fig. 2B, 3A), indicating a localized impact of ammonia.

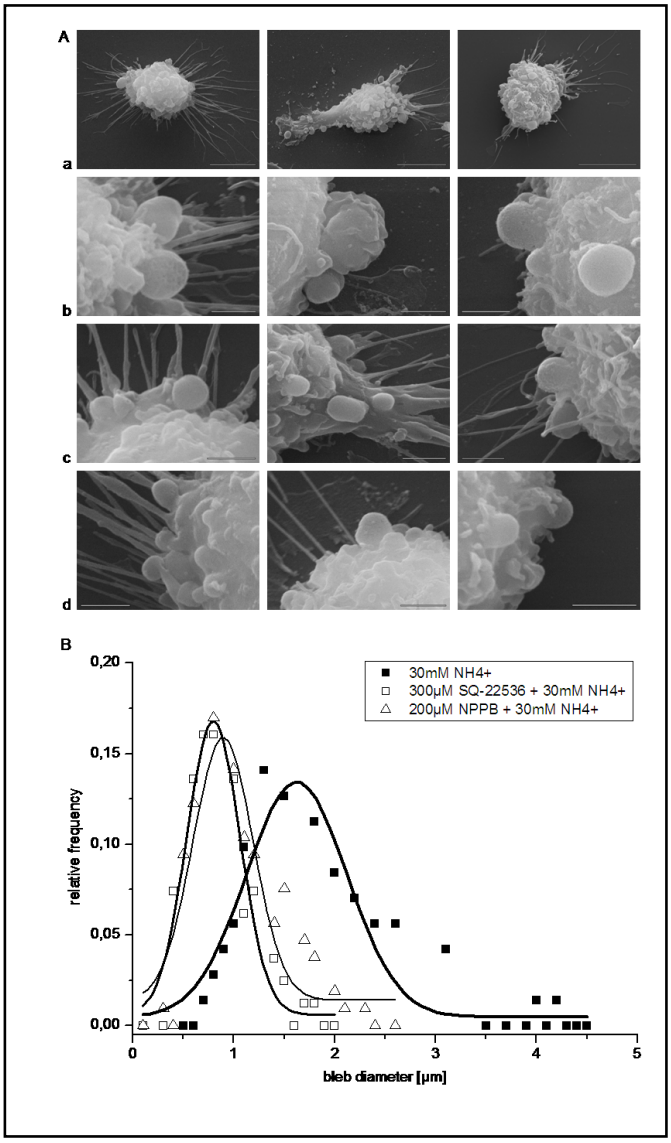

Fig. 3. SQ-22536 as well as NPPB suppresses ammonia-induced bleb formation. Cells were cultured in serum free medium containing 30mM ammonia for 25 minutes and then prepared for scanning electron microscopy. (A) Representative examples of cells cultured in the absence (a, b) or presence of SQ-22536 (300µM) (c) or NPPB (200µM) (d). Note that cells cultured in SQ-22536 or NPPB have smaller blebs than cells cultured in the absence of these compounds. a: Scale bar, 10µm; b, c, d: Scale bar, 2µm. (B) Frequency distribution of bleb diameter of cells cultured in the absence or presence of SQ-22536 (300µM) or NPPB (200µM). Most ammonia-induced blebs had a diameter of 1.8 ± 0.8µm (n = 10 cells). SQ-22536 (n = 10 cells) and NPPB (n = 10 cells) decreased ammonia-induced blebs to a diameter of 0.9 ± 0.3µm and 1.2 ± 0.5µm, respectively.

Each individual bleb was short-lived and lasted about 60 seconds. Assuming a hemisphere, most blebs arose to a volume of 1.5fL (diameter 1.8 ± 0.8µm; 10 cells) (Fig. 3B) until they retracted and vanished. Although the cell

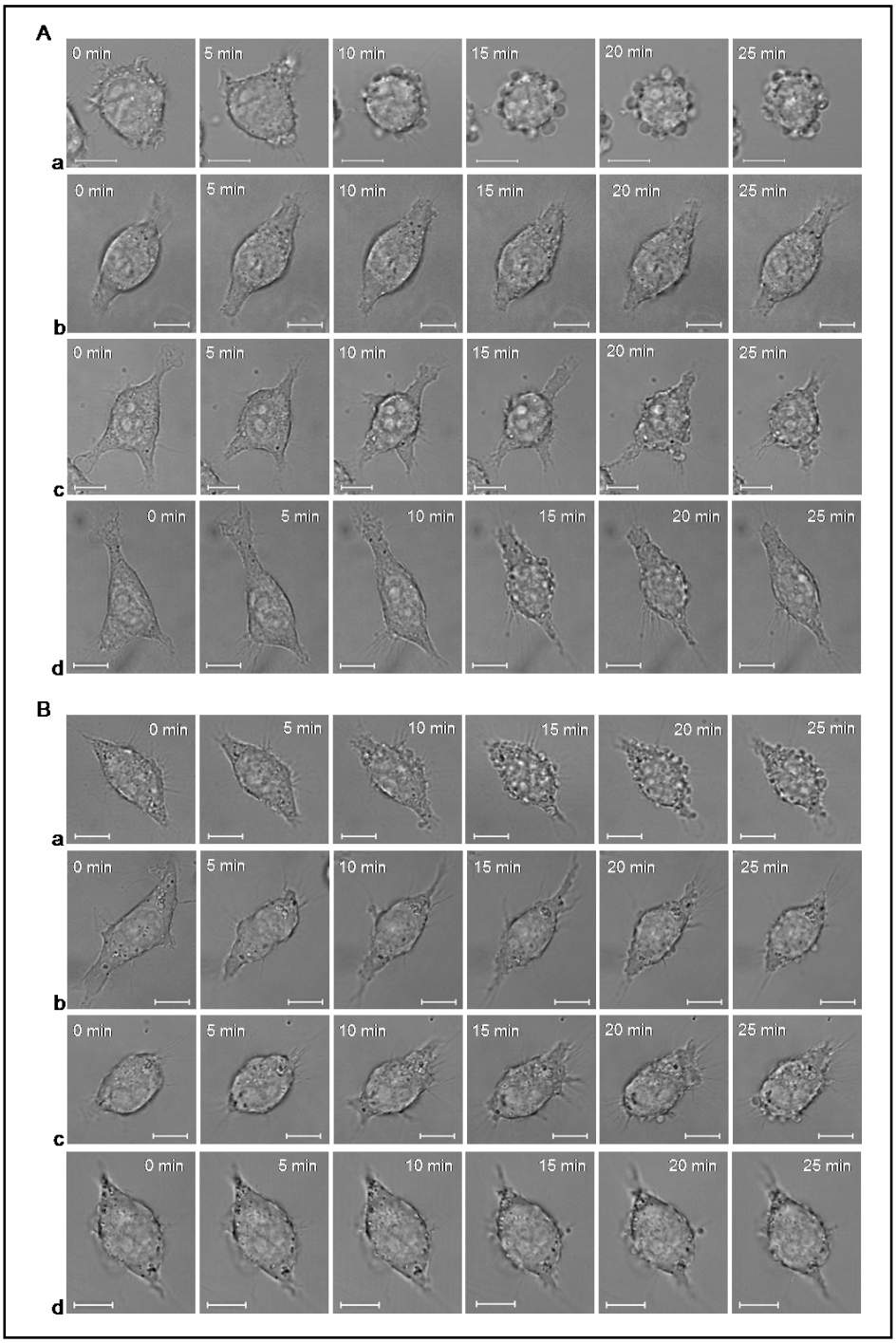

Fig. 4. Blockade of adenylyl cyclase, PKA, and Cl channels suppress ammonia-induced bleb formation. Cells were superfused for 25 minutes with serum-free medium supplemented with ammonia in the absence or presence of adenylyl cyclase, PKA, or Cl channel inhibitors and visualized by time-lapse confocal microscopy. (A) Inhibition of adenylyl cyclase with SQ-22536 (300µM) (b) and PKA with H-89 (1µM) (c) and Rp-cAMPs (10µM) (d) suppresses cell blebbing induced by ammonia (30mM) (a). (B) Blockade of Cl channels with DIOA (100µM) (b), flufenamic acid (200µM) (c), and NPPB (200µM) (d) inhibits membrane blebbing induced by ammonia (30mM) (a). Scale bar, 10µm.

body was covered with multiple protrusions, the blebs did not fuse.

The latency between ammonia application and bleb formation, number of blebbing cells as well as number of blebs per cell depended on the concentration of ammonia. Analysis of time-lapse movies revealed that 3mM ammonia initialized blebbing after about 15 minutes, 10mM after about 10 minutes, and 30mM after about 5 minutes (Fig. 4). Following 25 minutes of superfusion with 3mM, 10mM, and 30mM ammonia, about 19 ± 3% (n = 44), 37 ± 3% (n = 46), and 60 ± 3% (n = 41) of the cells, respectively, were blebbing (Fig. 5). The basal rate of blebbing was about 1.5%. Evaluation of blebbing at the single cell level via a blebbing index revealed a similar temporal pattern (Fig. 5).

Next, we evaluated the impact of adenylyl cyclase and PKA on ammonia-induced bleb formation (Fig. 4). Superfusion of BV-2 cells with SQ-22536 (300µM), an inhibitor of adenylyl cyclase, delayed bleb formation, decreased the number of blebbing cells, reduced the number

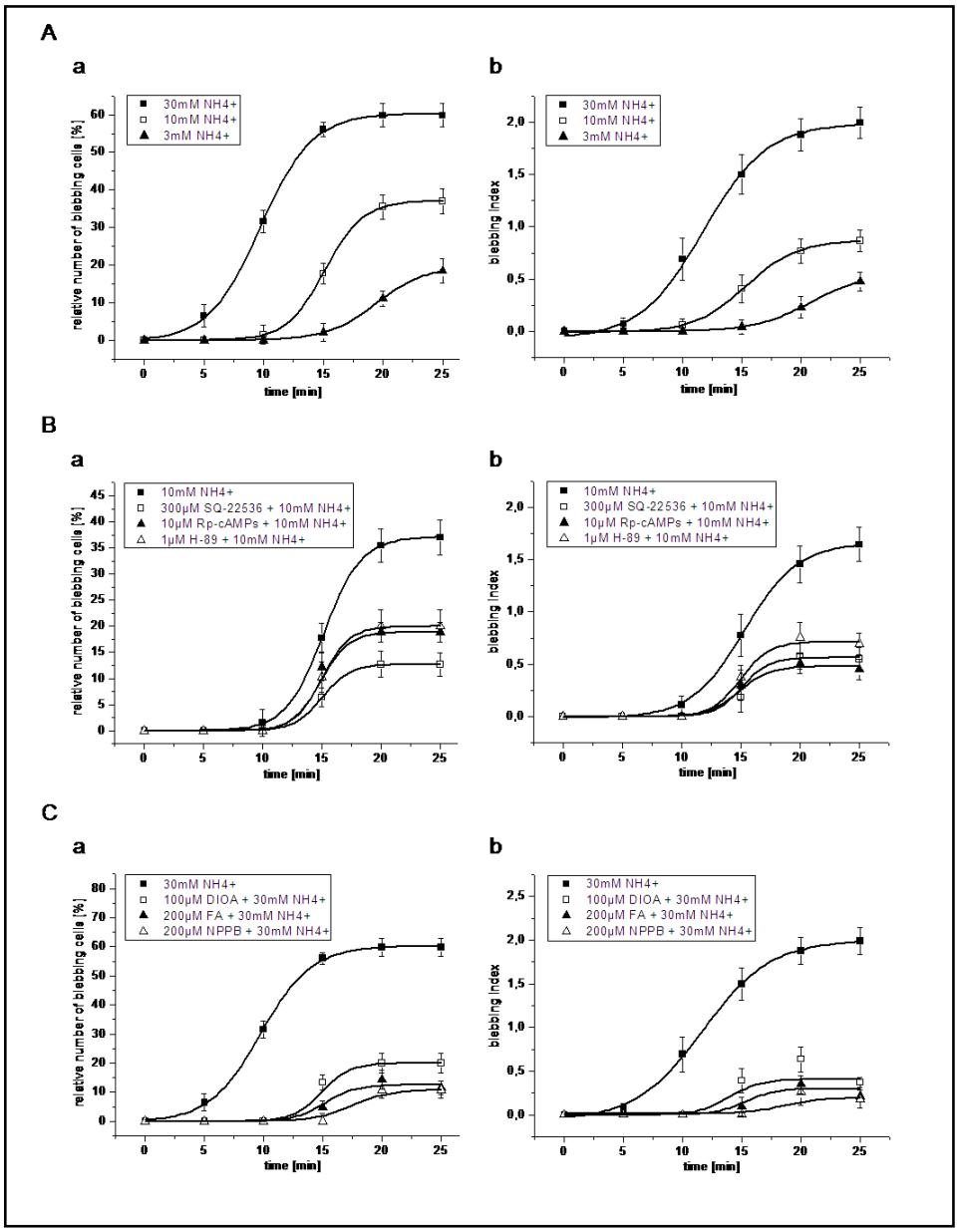

Fig. 5. Inhibition of adenylyl cyclase, PKA, and Cl channels suppress ammonia-induced bleb formation. Cells were cultured in serum-free media supplemented with ammonia for 5, 10, 15, 20, and 25 minutes. At each of these time points, the number of blebbing cells was determined and the blebbing index (see Material and Methods) was calculated and normalized. Each data point represents the mean ± SD of about 40 cells. (A) Increasing the ammonia concentration from 3mM to 10mM and 30mM accelerates bleb formation (a, b), increases the number of blebbing cells (a) and enhances the number of blebs per cell (b). (B) Inhibition of the adenylyl cyclase with SQ-22536 (300µM) or PKA with H-89 (1µM) or Rp-cAMPs (10µM) slowed down bleb formation (a, b), decreased the number of blebbing cells (a), and reduced the number of blebs per cell (b) induced by 10mM ammonia. (C) Blockade of Cl channels with DIOA (100µM), flufenamic acid (FA) (200µM), or NPPB (200µM) diminished the number of blebbing cells (a) as well as the number of blebs per cell (b) induced by 30mM ammonia.

of blebs per cell, and the maximum volume of single blebs. Cells exposed to SQ-22536 (300µM) postponed ammonia-induced bleb formation by about five minutes. 25 minutes after application of 10mM and 30mM ammonia, respectively, in the presence of SQ-22536, only 13 ± 2% (n = 38) and 25 ± 3% (n = 33) of the cells, respectively, showed bleb formation (Fig. 5). Cells treated with ammonia in the presence of SQ-22536 did produce significantly smaller protrusions than control cells exposed to ammonia only (Fig. 3). The average volume of the bleb was approximately 0.2fL (diameter 0.9 ± 0.3µm; 10 cells).

Similar to the experiments using SQ-22536, the inhibitors of PKA activity, Rp-adenosine 3',5'-cyclic monophosphorothioate triethylamine salt (Rp-cAMPs) and *N*-[2-(*p*-bromocinnamylamino)ethyl]-5-isoquinolinesulfonamide (H-89), delayed bleb formation, decreased the number of blebbing cells, the number of blebs per cell and the blebbing index as well as decreased the volume of single blebs (Fig. 5). Cells that displayed blebbing started to bleb later and blebbed only slightly. Rp-cAMPs (10µM) in the presence of 10mM (n = 35) and 30mM (n = 31) ammonia, respectively, suppressed ammonia-triggered bleb formation to 19 ± 2% and 33 ± 3%, respectively. Superfusion of BV-2 cells with H-89 (1µM) showed similar suppressing effects (10mM: n = 32; 30mM: n = 36).

Exposure of BV-2 cells to the cAMP analogues, 8-bromoadenosine 3',5'-cyclic monophosphate (8-Br-cAMP) (300µM) or Sp-adenosine 3',5'-cyclic monophosphorothioate (Sp-cAMP) (30µM), induced

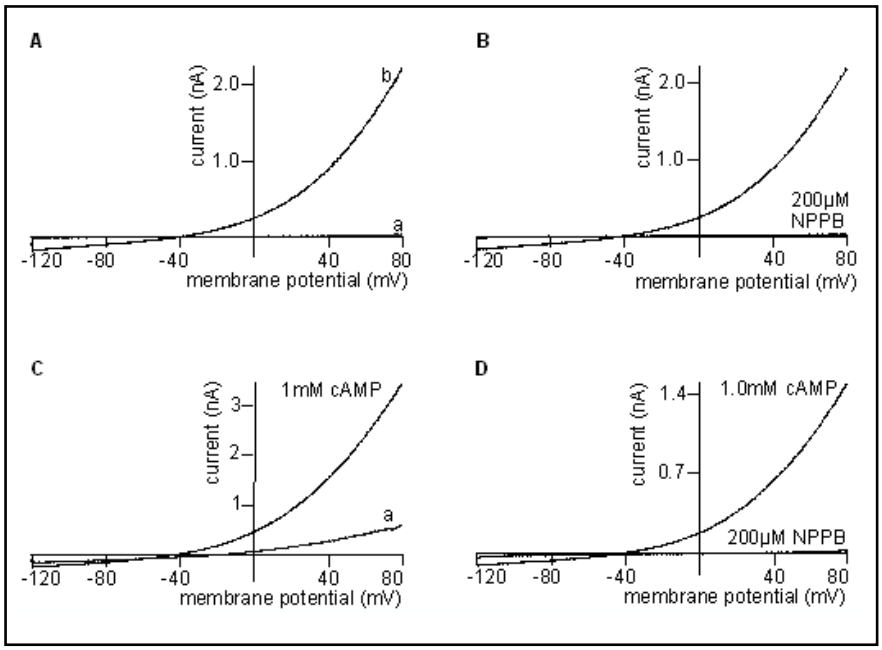

Fig. 6. Swelling-activated Cl^- current and cAMP-dependent Cl^- current. Current was recorded during a 400ms voltage ramp from -120 to +80mV separated by 5 seconds. The holding potential was 0mV. In (A) and (B), the current was evoked under hypotonic conditions (60% extracellular solution) and in (C) and (D), the cell was dialyzed with 1mM cAMP under normotonic conditions. Although the Nernst equation predicts E_{Cl} = -71mV (assuming 60% extracellular solution), the actual reversal potential is about -41mV. Assuming that the Cl channel is permeant to L-aspartate, the main anion in the intracellular solution, the calculated reversal potential is -40mV (E_{rev} = 58 log {[6mM + (0.1 x 150mM)]/102.3mM}, where "0.1" is the permeability ratio for L-aspartate and "102.3mM" is the Cl^- concentration of the hypotonic extracellular solution). (A) Representative ramp current traces recorded in normotonic saline (a) and 60% saline (b) during a voltage ramp from -120mV to +80mV. (B) The current induced by 60% saline was blocked with NPPB (200µM). (C) Cells dialyzed with cAMP showed already at the beginning of the recording a moderate Cl^- current ("a"). This current was not detectable when the cell was perfused with cAMP-free internal solution. The second trace ("1mM cAMP") visualizes the maximum current. (D) cAMP-dependent current was suppressed by NPPB (200µM).

blebbing after about three hours. This long latency might indicate that ammonia triggers several signalling pathways and cAMP enhances at least one of them.

Taken together, bleb formation in BV-2 cells is promoted by a cAMP-dependent pathway. These results confirm our previous finding [10] that ammonia-induced apoptosis is mediated via cAMP signalling pathway and indicates that cAMP already plays a critical role in the initial stages of this programmed cell death.

Blockade of chloride channels inhibits ammonia-induced blebbing

In microglia, like in other cell types, Cl channels participate in volume regulation [23-25]. Therefore, we studied the impact of the Cl^- conductance blockers, [(dihydroindenyl)oxy]alkanoic acid (DIOA), flufenamic acid and NPPB, on bleb formation induced by ammonia.

BV-2 cells were superfused with DIOA (100µM), flufenamic acid (200µM), or NPPB (200µM) in the presence of ammonia (30mM). Cells that showed bleb formation started to bleb later, blebbed only slightly, and partially stopped to bleb at the end of the experiment (Fig. 4). After 25 minutes of exposure to ammonia (30mM) in the presence of DIOA (100µM), an inhibitor of KCl cotransporters and swelling-activated Cl channels [13], only 20 ± 3% of the cells (n = 37) displayed membrane blebbing (Fig. 5). Flufenamic acid (200µM) and NPPB (200µM), blockers of swelling-activated Cl channels, exerted similar effects, suppressing ammonia-induced bleb formation to 12 ± 2% (n = 40) and 11 ± 3% (n = 44), respectively (Fig. 5). BV-2 cells exposed to ammonia in the presence of NPPB formed significantly smaller blebs than control cells treated with ammonia only (Fig. 3). The average volume of the cell protrusion was about 0.5fL (diameter 1.2 ± 0.5µm; 10 cells).

Taken together, blockade of Cl^- conductance prevented membrane blebbing in ammonia-treated BV-2 cells, indicating that the formation of cell blebs is mediated by Cl channel activity.

cAMP activates a chloride conductance

Because we found in the present study that inhibition of adenylyl cyclase and PKA activity, respectively, as well as blockade of Cl channels suppressed bleb formation and other studies indicated that intracellular cAMP activates swelling-activated Cl channels [14, 15], we compared electrophysiological and pharmacological properties of Cl^- currents triggered either by cell swelling in a hypotonic solution or by perfusion of the cell with cAMP or the catalytic unit of PKA.

Whole-cell current was monitored either during voltage ramps from -120mV to +80mV or voltage steps. To avoid contaminations from voltage-gated K channels, the membrane potential was clamped to 0mV. Under

normotonic conditions, we did not detect any current in addition to the leak current. Superfusion of BV-2 cells with a hypotonic solution elicited an outwardly rectifying current (Fig. 6A, B). The current reversed at -41.1 ± 4.5mV (n = 7). This is about 30mV more positive than expected from a perfect Cl^- selective ion channel (E_{Cl} = -71mV, assuming a hypotonic solution) and indicates permeability of additional anions, like L-aspartate (see figure legend; Fig. 6). The maximum current density at 80mV was 95.7 ± 31.1nA/pF. Stimuli with voltage steps revealed a non-inactivating current (not shown). Osmotically activated Cl channels were sensitive to NPPB and flufenamic acid. Application of NPPB (200µM) and flufenamic acid (200µM) completely suppressed the outwardly rectifying current (Fig. 6B).

Intracellular perfusion of BV-2 cells with cAMP evoked an outwardly rectifying current under normotonic conditions (Fig. 6C, D). Using 300µM, the current density was 30.3 ± 13.6nA/pA (n = 5) and using 1mM cAMP the current density was 54.5 ± 41.7nA/pA (n = 10) at 80mV. The Cl^- current did not inactivate during a 100ms voltage step. Application of NPPB (200µM) and flufenamic acid (200µM) completely suppressed the current (Fig. 6 D). The membrane capacitance did not show any detectable difference during the development of the Cl^- current. Increasing the extracellular osmolarity from 300 to 330mosmol prevented the development of a Cl^- current in cells perfused with cAMP (1mM; n = 6) or superfused with the membrane permeable db-cAMP (300µM: n = 8; 1mM: n = 10).

To distinguish outward rectification due to the Cl^- gradient (Goldman rectification) from intrinsic properties of the ion channel, we did additional experiments using isoosmotic symmetrical Cl^- solutions. Isoosmotic symmetrical Cl^- solutions favour activation of a Cl^- conductance. In the absence of intracellular cAMP, some cells showed a small outward current (0.9 ± 0.5nA at + 80mV; n = 7). Perfusion of the cell with 1mM cAMP provoked a non-linear current (Fig. 7) (3.3 ± 1.5nA at +80mV, n = 10). Intracellular perfusion of the cell with cAMP not only evoked a Cl^- conductance but also increased membrane capacitance (Fig. 7C). These experiments indicate that the cAMP-dependent Cl^- channel has intrinsic nonlinear properties and causes a small increase in cell volume.

Perfusion of the cell with the enzymatic subunit of PKA (300 units) evoked an outwardly rectifying Cl^- current (Fig. 8). The current density ranged between 13.6 and 139.0nA/pA (52.2 ± 48.8nA/pA; n = 8). Furthermore, the current was suppressed by NPPB (200µM) and flufenamic acid (200µM) (Fig. 8C, D).

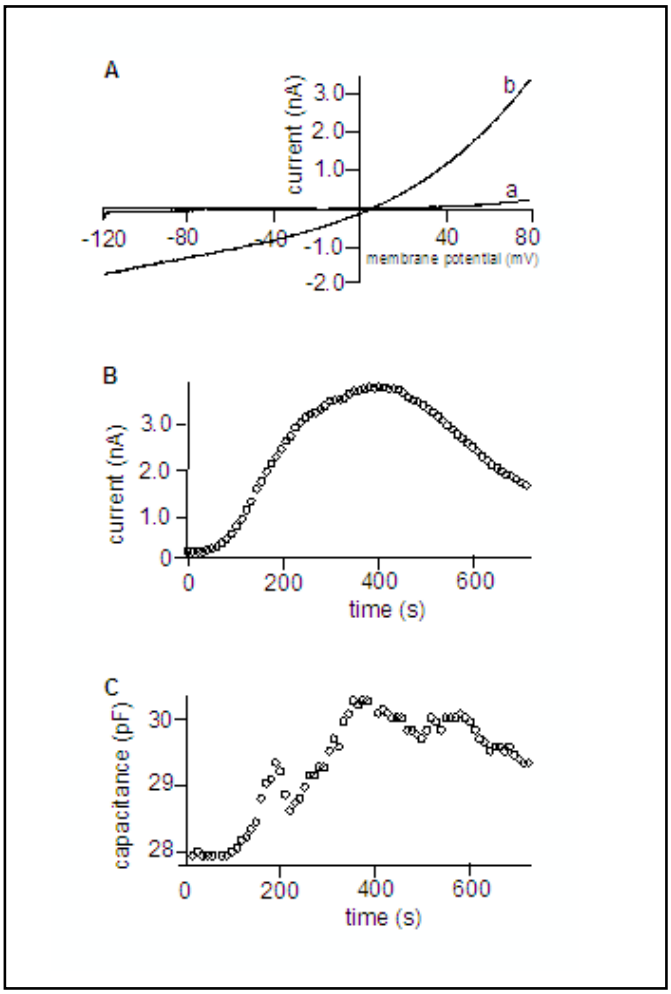

Fig. 7. Parallel development of cAMP-dependent Cl^- current and membrane capacitance. cAMP (1mM) was delivered via the patch pipette. Recording was performed with isoosmotic symmetrical Cl^- solutions. (A) Representative current traces collected 10 seconds (a) and 370 seconds (b) after break in. (B) Development of cAMP-dependent Cl^- current. A voltage ramp was delivered every 10 seconds and the current amplitude at +80mV was plotted versus time. (C) Membrane capacitance increased and decreased, respectively, parallel to the Cl^- current from the cell shown in (B).

The swelling-activated Cl^- current and the cAMP-dependent Cl^- current behaved similarly, each showing an outward rectification, time-independent gating, and sensitivity to NPPB and flufenamic acid, respectively. The ratio of the outward current at 80mV and the inward current at -80mV was 28.7 ± 9.2 (n = 8) in swelling-activated current, 33.4 ± 11.3 in cAMP-induced current (1mM cAMP), and 12.8 ± 3.8 in PKA-dialyzed cells using asymmetrical Cl^- distribution.

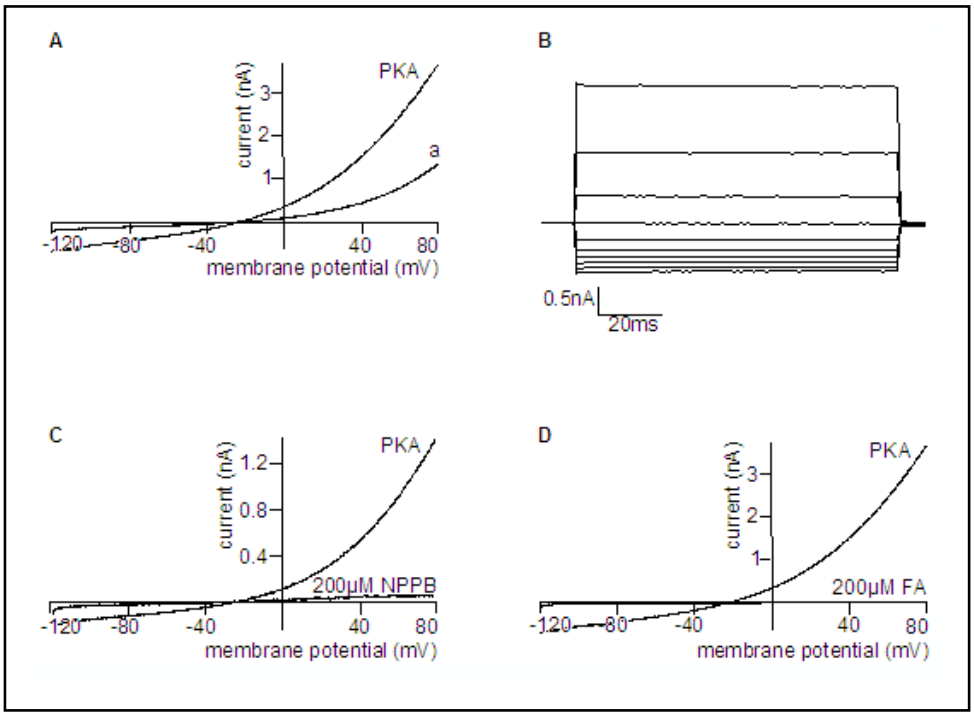

Fig. 8. Catalytic subunit of PKA induces a Cl^- current. Cells were bathed in normotonic saline and dialyzed with the catalytic subunit of PKA (300 units). Currents were either elicited during voltage ramps from -120mV to +80mV or during voltage steps from -120mV to +60mV in 20mV increments delivered by 5 seconds. (A) Cl^- ramp currents at the beginning ("a") and maximum ("PKA") of the current development. Cells dialyzed with the catalytic subunit of PKA showed a moderate Cl^- current already at the beginning of the recording. (B) Cl^- currents during voltage steps of a cell maximally activated with the catalytic subunit of PKA. PKA-induced current was suppressed by NPPB (200µM) (C) as well as flufenamic acid (FA) (200µM) (D).

Ammonium evokes a Cl^- current

The measurements were performed in isoosmotic symmetrical Cl^- solutions in the absence and presence of 5mM ammonium. Superfusion of the cell with ammonium induced an outwardly rectifying current (1.7 ± 1.1nA, n = 3) which had a reversal potential of 3.2 ± 2.9mV (Fig. 9). The ammonium-induced current was partially blocked by 200µM flufenamic acid. According to the outward rectification, reversal potential close to 0mV, and sensitivity to flufenamic acid, we assume that ammonium activates a cAMP-dependent or swelling-activated Cl^- current similar to the one described in the previous section of this study, although a flufenamic acid-insensitive outward rectifying current could also be observed.

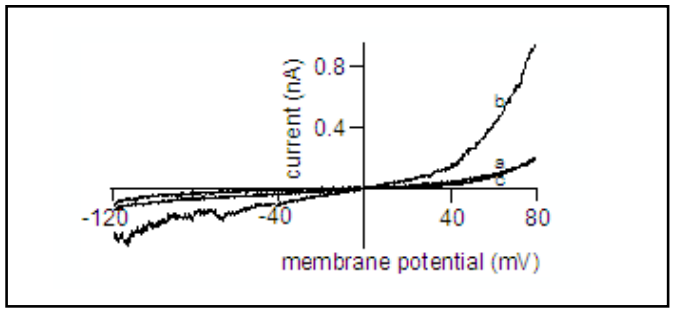

Fig. 9. Ammonium activates a Cl^- current. Exposure of a cell to ammonium (5mM) in isoosmotic symmetrical Cl^- solutions caused an outwardly rectifying current. Ramp currents were recorded every 10 seconds before (a) and after (b) superfusion with 5mM ammonium. Flufenamic acid (200µM) in the presence of ammonium suppressed the current (c).

Discussion

Local cell protrusions are a common phenomenon in a diversity of cellular responses, including formation of engulfment pseudopodia upon phagocytosis of particles [9], extension of lamellipodia to allow migration [13], and formation of blebs during an early phase of apoptosis [10]. Although membrane blebbing is a familiar apoptotic feature, the mechanism of bleb formation has attracted less attention. Some studies favour a hydrostatic model [16, 26], whereas other studies suggest an osmotic model in bleb formation [27]. Regardless of the model, regulation of the actin skeleton is in the focus of most studies on cell blebbing [28, 29]. In the present study, we include cAMP-dependent Cl channels to the actin model of bleb formation. Because BV-2 cells are electrophysiologically well characterized [8, 30] and show biologically significant aspects of local swellings, like formation of lamellipodia and elongated cell processes, engulfment of particles or cell blebbing during apoptosis [8-13], we selected this cell type as a model for our study.

Microglial cells, including BV-2 cells, express swelling-activated Cl channels [8, 13, 23, 30]. This Cl channel is electrophysiologically characterized by a time- and voltage-independent gating, a single channel conductance of 1 - 3pS as well as an outwardly rectifying current and

pharmacologically by its sensitivity to NPPB, 4-acetamido-4V-isothiocyanatostilbene-2,2Vdisulfonic acid (SITS), 4,4V-diisocyanatostilbene-2,2Vdisulfonic acid (DIDS), flufenamic acid, the indanylalkanoic acid, IAA-94, and DIOA [8, 13, 23].

In microglial cells, activation of Cl channels has been associated with induction of ramification [8, 11], migration [31], formation of lamellipodia [13], formation of engulfment pseudopodia [9], and formation of blebs (present study). The temporal sequence in formation of local protrusions and Cl channel activation can be seen either as (1) a localized cell swelling followed by an activation of Cl channels or (2) activation of Cl channels followed by a localized swelling. Because suppression of adenylyl cyclase activity suppresses bleb formation and cAMP activates a Cl^- conductance, we assume that exogenous or endogenous factors trigger the formation of an intracellular messenger, like cAMP, which promotes Cl channel activation followed by an influx of water and localized cell swelling.

The life cycle of a bleb consists of nucleation (detachment of the plasma membrane from the submembranal cytoskeleton), expansion, maturation, and retraction [16, 26, 32]. Our study contributes experimentally to the interpretation of the expansion phase and provides predictions to the retraction phase of bleb formation. Whereas in the filamin-deficient melanoma cell line, M2, the endogenous continuous blebbing is attributed to intracellular hydrostatic pressure and redistribution of cytosol [16, 26], we assume that ammonia-induced bleb formation in BV-2 cells is related to an osmotically driven influx of water. We suggest that the expansion phase correlates with an activation of Cl channels. An exogenous factor, like ammonia, ignites adenylyl cyclase, and, consequently, promotes accumulation of cAMP. An increase in intracellular cAMP concentration favours the catalytic activity of PKA [10]. Phosphorylation facilitates opening of Cl channels and an influx of anionic osmolytes. Accordingly, activation of Cl channels is not a consequence of global cell swelling, but is the consequence of localized cell swelling. Actually, the contribution of Cl channels to cell blebbing could go beyond the expansion phase using the following argument. Influx and efflux of anionic osmolytes through Cl channels depend on the relative position of E_{Cl} to E_M. During the expansion phase, E_{Cl} is more negative than E_M and opening of the Cl channels results in an influx of Cl^- (equals an outward current), whereas during the retraction phase, E_{Cl} is less negative than E_M, forcing Cl^- out of the cell (equals an inward current). At the moment, it is not known whether

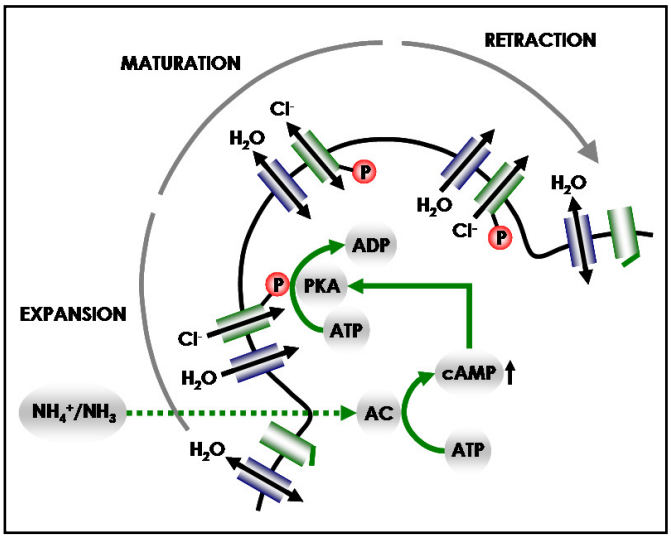

Fig. 10. Contribution of Cl^- conductance to expansion, maturation, and retraction of a bleb. The cartoon shows distinct phases of the life cycle of a bleb. We suggest that PKA-dependent phosphorylation of a Cl channel facilitates opening of this ion channel. Depending on the relative position of E_{Cl} to E_M, there is either an influx (E_{Cl} is more negative than E_M) or efflux of Cl^- (E_{Cl} is less negative than E_M). An influx of Cl^- is accompanied by an influx of water (expansion phase) and an efflux of Cl^- is accompanied by an efflux of water (retraction phase). During maturation, we assume that $E_{Cl} = E_M$ and, accordingly, the netto flux of Cl^- and water, respectively, is zero.

a shift in the relative position of E_{Cl} to E_M is due to a change in E_{Cl} or E_M. An accumulation of intracellular anionic osmolytes during the expansion phase predicts a shift towards a more depolarized membrane potential. An alternative possibility is an increase in K^+ conductance during blebbing. Accordingly, the membrane potential hyperpolarizes and E_M is more negative than E_{Cl}. In both speculative scenarios, E_M is positioned below E_{Cl} and anionic osmolytes diffuse out of the cell promoting retraction of the bleb. Our osmocentric view is intended to complement models based on the actin skeleton. Because ammonia modulates the intracellular pH, which in turn affects actin polymerization and depolymerization as well as Cl^- conductance [33, 34], the cAMP-dependent effects reported in the present study may be accompanied by pH-dependent mechanisms.

Whether cAMP-dependent Cl channels are identical to swelling-activated Cl channels is still a matter of debate [14, 15]. Our preliminary comparison of swelling-activated and cAMP-dependent Cl^- currents in microglial cells suggests similar properties in outward rectification, kinetics of the current during voltage steps, and sensitivity to Cl channel blockers. However, even if these

Cl channels are identical, cAMP-dependent processes do only facilitate opening of Cl channels because intracellular cAMP promotes Cl^- current at an extracellular osmolarity of about 300mosmol but not at 330mosmol. In addition to directly modulating Cl channels via PKA-mediated phosphorylation of Cl channels, cAMP also modulates actin polymerization and depolymerization [35], which has an impact on Cl channel activation [36, 37].

Abbreviations

8-Br-cAMP (8-bromoadenosine 3',5'-cyclic monophosphate); cAMP (cyclic adenosine 3',5'-monophosphate); DIDS (4,4V-diisocyanatostilbene-2,2Vdisulfonic acid); DIOA ([(dihydroindenyl)oxy]alkanoic acid); DMEM (Dulbecco's modified Eagle's medium); E_C, (equilibrium potential of Cl^-); E_M (membrane potential); E_{rev} (reversal potential); H-89 (*N*-[2-(*p*-bromocinnamylamino)ethyl]-5-isoquinolinesulfonamide); NPPB (5-nitro-2-(3-phenylpropylamino)benzoic acid); PKA (protein kinase A); Rp-cAMPs (Rp-adenosine 3',5'-cyclic monophosphorothioate triethylamine salt); RVD (regulatory volume decrease); SITS (4-acetamido-4V-isothiocyanatostilbene-2,2Vdisulfonic acid); Sp-cAMP (Sp-adenosine 3',5'-cyclic monophosphorothioate).

Acknowledgements

Nina Svoboda was supported by a grant from the Austrian Academy of Sciences (DOC-fFORTE No. 22308) and Sylvia Prütting by grants from the 4SC AG (Martinsried), the Land Baden-Württemberg (1423/74) and the DFG (Gr848/14-1). We would like to thank Katharina Ruff for technical assistance, Nikolaus Bresgen for discussions on apoptosis, and Luette Forrest for constructive comments on the manuscript.

References

1 Del Rio-Hortega P: Microglia; in Penfield W (ed): Cytology and cellular pathology of the nervous system. New York, PB Hoebaer, 1932, pp 483–534.

2 Kreutzberg GW: Microglia: a sensor for pathological events in the CNS. Trends Neurosci 1996;19:312–318.

3 Ladeby R, Wirenfeldt M, Garcia-Ovejero D, Fenger C, Dissing-Olesen L, Dalmau I, Finsen B: Microglial cell population dynamics in the injured adult central nervous system. Brain Res Brain Res Rev 2005;48:196–206.

4 Davalos D, Grutzendler J, Yang G, Kim JV, Zuo Y, Jung S, Littman DR, Dustin ML, Gan WB: ATP mediates rapid microglial response to local brain injury in vivo. Nat Neurosci 2005;8:752–758.

5 Nimmerjahn A, Kirchhoff F, Helmchen F: Resting microglial cells are highly dynamic surveillants of brain parenchyma in vivo. Science 2005;308:1314–1318.

6 Franklin RJ: Why does remyelination fail in multiple sclerosis? Nat Rev Neurosci 2002;3:705–714.

7 Hauwel M, Furon E, Canova C, Griffiths M, Neal J, Gasque P: Innate (inherent) control of brain infection, brain inflammation and brain repair: the role of microglia, astrocytes, "protective" glial stem cells and stromal ependymal cells. Brain Res Rev 2005;48:220–233.

8 Eder C, Klee R, Heinemann U: Involvement of stretch-activated Cl^- channels in ramification of murine microglia. J Neurosci 1998;15:7127–7137.

9 Furtner T, Zierler S, Kerschbaum HH: Blockade of chloride channels suppresses engulfment of microspheres in the microglial cell line, BV-2. Brain Res 2007;1184:1–9.

10 Svoboda N, Zierler S, Kerschbaum HH: cAMP mediates ammonia-induced programmed cell death in the microglial cell line, BV-2. Eur J Neurosci 2007;25:2285–2295.

11 Zierler S, Kerschbaum HH: Blockade of chloride conductance antagonizes PMA-induced ramification in the murine microglial cell line, BV-2. Brain Res 2005;1039:162–170.

12 Zierler S, Klein B, Furtner T, Bresgen N, Luetz-Meindl U, Kerschbaum HH: Ultraviolet irradiation-induced apoptosis does not trigger nuclear fragmentation but translocation of chromatin from nucleus into cytoplasm in the microglial cell-line, BV-2. Brain Res 2006;1121:12–21.

13 Zierler S, Frei E, Grissmer S, Kerschbaum HH: Chloride influx provokes lamellipodium formation in microglial cells. Cell Physiol Biochem 2008;21:55–62.

14 Carpenter E, Peers C: Swelling- and cAMP-activated Cl^- currents in isolated rat carotid body type I cells. J Physiol 1997;503:497–511.

15 Meng XJ, Weinman SA: cAMP- and swelling-activated chloride conductance in rat hepatocytes. Am J Physiol 1996;271:C112–120.

16 Charras GT, Yarrow JC, Horton MA, Mahadevan L, Mitchison TJ: Non-equilibration of hydrostatic pressure in blebbing cells. Nature 2005;435:365–369.

17 Hamill OP, Marty A, Neher E, Sakmann B, Sigworth FJ: Improved patch-clamp techniques for high-resolution current recording from cells and cell-free membrane patches. Pflugers Arch 1981;391:85–100.
18 Kerschbaum HH, Negulescu PA, Cahalan MD: Ion channels, Ca2+ signaling, and reporter gene expression in antigenspecific mouse T cells. J Immunol 1997;159:1628–1638.
19 Lewis RS, Ross PE, Cahalan MD: Chloride channels activated by osmotic stress in T lymphocytes. J Gen Physiol 1993;101:801–826.
20 Marcaggi P, Coles J: Ammonium in nervous tissue: transport across cell membranes, fluxes from neurons to glial cells, and role in signalling. Prog Neurobiol 2001;64:157–183.
21 Felipo V, Butterworth RF: Neurobiology of ammonia. Prog Neurobiol 2002;67:259–279.
22 Tokuda S, Shimamoto C, Yoshida H, Murao H, Kishima G, Ito S, Kubota T, Hanafusa T, Sugimoto T, Niisato N, Marunaka Y, Nakahari T: HCO_3^--dependent pHi recovery and overacidification induced by NH_4^+ pulse in rat lung alveolar type II cells: HCO_3^--dependent NH_3 excretion from lungs? Pflugers Arch 2007;455(2):223–239.
23 Ducharme G, Newell EW, Pinto C, Schlichter LC: Small-conductance Cl^- channels contribute to volume regulation and phagocytosis in microglia. Eur J Neurosci 2007;26:2119–2130.
24 Eder C: Regulation of microglial behavior by ion channel activity. J Neurosci Res 2005;81:314–321.
25 Lang F, Busch GL, Ritter M, Voelkl H, Waldegger S, Gulbins E, Haeussinger D: Functional significance of cell volume regulatory mechanisms. Physiol Rev 1998;78:247–306.
26 Charras GT, Coughlin M, Mitchison TJ, Mahadevan L: Life and times of a cellular bleb. Biophys J 2008;94:1836–1853.
27 Harris A: Cell surface movements related to cell locomotion. CIBA Found Symp 1973;14:3–20.
28 Cunningham CC: Actin polymerization and intracellular solvent flow in cell surface blebbing. J Cell Biol 1995;129:1589–1599.
29 Mills JC, Stone NL, Erhardt J, Pittman RN: Apoptotic membrane blebbing is regulated by myosin light chain phosphorylation. J Cell Biol 1998;140:627–636.
30 Eder C: Ion channels in microglia (brain macrophages). Am J Physiol 1998;275:C327–C342.
31 Rappert A, Biber K, Nolte C, Lipp M, Schubel A, Lu B, Gerard NP, Gerard C, Boddeke HW, Kettenmann H: Secondary lymphoid tissue chemokine (CCL21) activates CXCR3 to trigger a Cl^- current and chemotaxis in murine microglia. J Immunol 2002;168:3221–3226.
32 Torgerson RR, McNiven MA: The actin-myosin cytoskeleton mediates reversible agonist-induced membrane blebbing. J Cell Sci 1998;111:2911–2922.
33 Baumgartner M, Patel H, Barber DL: Na(+)/H(+) exchanger NHE1 as plasma membrane scaffold in the assembly of signaling complexes. Am J Physiol Cell Physiol 2004;287(4):C844–C850.
34 Frantz C, Barreiro G, Dominguez L, Chen X, Eddy R, Condeelis J, Kelly MJ, Jacobson MP, Barber DL: Cofilin is a pH sensor for actin free barbed end formation: role of phosphoinositide binding. J Cell Biol 2008;183(5):865–879.
35 Beene DL, Scott JD: A-kinase anchoring proteins take shape. Curr Opin Cell Biol 2007;19:192–198.
36 Lascola CD, Kraig RP: Whole-cell chloride currents in rat astrocytes accompany changes in cell morphology. J Neurosci 1996;16:2532–2545.
37 Ullrich N, Sontheimer H: Cell cycle-dependent expression of a glioma-specific chloride current: proposed link to cytoskeletal changes. Am J Physiol 1997;273:C1290–C1297.